Design of W-band high-order mode extended interaction klystron based on novel multi-gap cavity

XIE Bing-Chuan[1,2], ZHANG Rui[1*], WANG Huan-Huan[3], WANG Yong[1,2], GENG Zhi-Hui[1],

LIAO Yun-Feng[1], YANG Xiu-Dong[1]

（1. Key Laboratory of Science and Technology on High Power Microwave Sources and Technologies, Aerospace Information Research Institute, Chinese Academy of Sciences, Beijing 100190, China；
2. School of Electronic, Electrical and Communication Engineering, University of Chinese Academy of Sciences, Beijing 100049, China；
3. Center of Materials Science and Optoelectronics Engineering, School of Optoelectronics, University of Chinese Academy of Sciences, Beijing 100049, China）

Abstract：A novel resonator has been proposed for the klystron that operates at TM_{310} mode. The electric fields of both the middle cavity and the side cavity are effectively enhanced by discretizing the field in the side cavity. The novel resonator demonstrates a higher characteristic impedance than the traditional barbell shape cavity when both cavities operate at TM_{310} mode. Sensitivity analysis has been performed on these two kinds of cavities. Moreover, an RF circuit in the W-band has been designed based on the proposed novel cavity. The RF circuit can achieve a high gain of 52. 4 dB and a peak output power of 7. 8 kW when 45 mW input power is injected. The circuit is driven by a 25 kV and 2 A pencil beam. The electronic efficiency and 3-dB bandwidth are 15. 6% and 120 MHz, respectively.

Key words：extended interaction klystron（EIK）, high-order mode cavity, field discretizing, barbell shaped cavity, sensitivity analysis

基于新型多间隙谐振腔的 W 波段高次模式扩展互作用速调管设计

谢冰川[1,2]，张　瑞[1*]，王欢欢[3]，王　勇[1,2]，耿志辉[1]，廖云峰[1]，杨修东[1]
（1. 中国科学院 空天信息创新研究院 高功率微波源与技术重点实验室，北京 100190；
2. 中国科学院大学 电子电气与通信工程学院，北京 100049；
3. 中国科学院大学 材料科学与光电技术学院，北京 100049）

摘要：提出了一种工作在 TM_{310} 模式下的用于高次模式速调管的新型谐振腔。通过对侧腔电场的离散化，可以有效地增强中间腔和侧腔的电场。当两腔均工作在 TM_{310} 模式时，新型谐振腔的特性阻抗均高于传统的哑铃型腔。对两种腔体进行了尺寸敏感性分析。在此基础上，设计了一个 W 频段的射频电路。当向射频电路注入 45 mW 的输入功率时，获得了 52.4 dB 的高增益和 7.8 kW 的峰值输出功率。互作用电路由 25 kV、2 A 的圆形电子注驱动。该互作用电路的电子效率和 3-dB 带宽分别为 15.6% 和 120 MHz。

关　键　词：扩展互作用速调管；高次模腔；场离散化；哑铃型腔；敏感性分析

中图分类号：TN122　　文献标识码：A

Introduction

Klystron is a kind of high-power microwave device that plays a critical role in remote sensing, imaging, high-power radar, and other applications. The extended interaction klystron (EIK) has high output power, high gain, tolerable bandwidth, and most importantly, excellent spectrum purity. EIK was first proposed by Chodorow and Kulke, et al[1]. The EIK combines the advantages of klystrons and traveling wave tubes (TWT). The multi-gap cavity used in the EIK has a high characteristic impedance, which can effectively shorten the length of the interaction circuit. Therefore, it has received extensive attention in high frequency bands.

In 30-300 GHz, the EIK has shown great power potential. In 2007, CPI (Communications & Power Industries Canada Inc) revealed a variety of EIKs that could operate at frequencies up to 280 GHz[2]. In the W-band, CPI has demonstrated an EIK that could generate an output power of 3 kW. However, as the frequency increases, the device becomes incredibly small. The power capacity decreases rapidly. The klystron using a sheet beam has been proposed to increase the total current that can be transmitted at a given voltage[3]. In the W band, two sheet beam klystrons have been successfully developed. The NRL (The Naval Research Laboratory) reported a W-band extended interaction klystron, which used a strong uniform magnetic field to focus sheet beam in 2014[4]. The total current in the beam tunnel was 3.6 A and the beam voltage was 20 kV. The peak output power was 7.5 kW with an electronic efficiency of 10.4%. In addition, researchers from the University of California at Davis (UC Davis) have also demonstrated a high-power W-band klystron, which can generate a peak output power of 56.3 kW[5,6]. The klystron is driven by a 74 kV and 3.6 A sheet beam. The electronic efficiency is 21%. The sheet beam klystron exhibits great power potential. However, the optical design of the sheet beam is complex, and the focusing of the sheet beam is difficult[7,8]. Most importantly, the efficiency of the sheet beam klystron is unsatisfactory.

Moreover, simultaneously arranging multiple pencil beams in the klystron can increase the output power and reduce the beam voltage[9-11]. However, in the W band, the device becomes very small, and the circular ring cavity used in the multi-beam klystron becomes difficult to fabricate. To accommodate modern high-precision planar machining techniques such as UV LIGA and WEDM, a klystron using a planar arrangement of multiple electron beams has been proposed[12]. However, the opticcal design of a planar multi-beam klystron is also a problem, and such a planar multi-beam design requires extremely high cathode loading (50-10 A/cm²) because of its extremely narrow electron beam spacing.

Designing a klystron with a single pencil beam and planar resonators is more practical in high-frequency bands. In the high-frequency band, high-precision processing mainly relies on WEDM, X-Ray Lithography, and UV LIGA. These machining techniques can maintain precision machining up to 1.1 THz[13]. An extended interaction klystron with resonators operating in a high-order mode has been proposed to increase the total current in the klystron that operates at high-frequency bands[14]. In Ref. [14], the designed 0.34 THz klystron can accommodate a total current of 0.3 A. However, the gain of the klystron is only 43 dB due to the various losses and the low characteristic impedance of the high-order mode cavity used.

In this paper, a novel resonator has been proposed for the klystron that operates in a high-order mode. The resonator can operate in the true $TM_{310-2\pi}$ mode to generate a stronger field in interaction gaps. Therefore, the proposed resonator has a higher characteristic impedance. As a result, efficiency and gain are improved. An interaction circuit with 52.4 dB gain and 15.6% electronic efficiency has been designed. The novel cavity remains a planar structure, which is suitable for modern high-precision planar machining techniques.
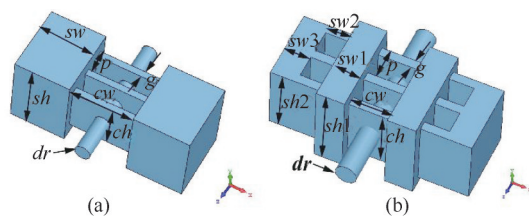

Fig. 1   Diagram of cavities (a) the traditional ladder type cavity, (b) the novel cavity

图 1   腔体示意图(a) 传统的梯形腔,(b)新型腔

1   Study of novel cavity

The conventional ladder type cavity used in high-order mode klystron is shown in Fig. 1(a). In Fig. 1, the drift tube radius is represented as *dr* and the period of the gap is represented as *p*. The gap axial length is represented as *g*. The TM_{310} mode distribution of the ladder type cavity is shown in Fig. 2(a). The reverse field in the side cavity is joined together, which is a waste of energy in the cavity. In order to use the field in the cavity efficiently, we proposed a novel cavity [see Fig. 1(b)]. The special structure designed in the novel cavity is to realize the real TM_{310} mode distribution. The TM_{310} mode distribution of the novel cavity is shown in Fig. 2(b). The reverse fields in both side cavities have been split into three peaks. The field becomes more concentrated. The two reverse field peaks are well confined in the side gaps [see Fig. 2(b)] instead of filling the whole side cavity [see Fig. 2(a)]. Figure 3 shows the axial field distribution at center gaps and side cavities of these two kinds of cavities. The novel cavity has a stronger field both in the central gaps and in the side cavities. Parameters of the two cavities are listed in Table 1. Figure 4 shows the transverse distribution of the axial electric field of the novel and traditional one.

The characteristic impedance (R/Q) and coupling coefficient (M) of the resonator are important parameters in the design of klystron and can be calculated from equa-
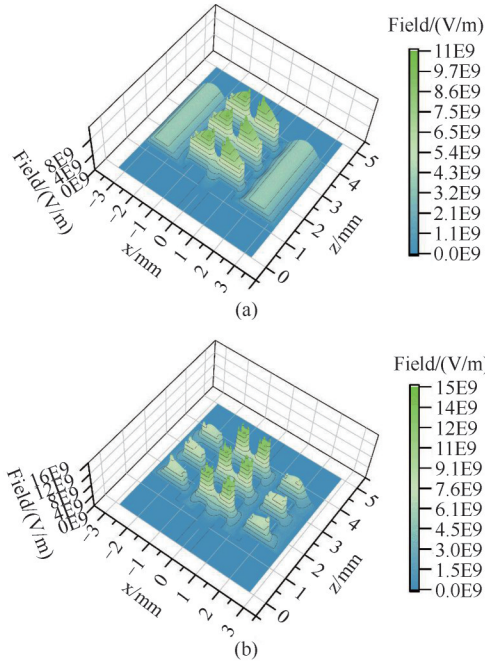
Fig. 2 TM_{310} mode distribution in xOz plane of two different cavities, (a) the traditional ladder type cavity, (b) the novel cavity

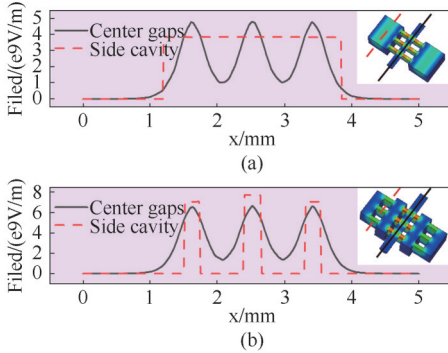图2 TM_{310} 模式在xOz平面上的分布示意图,(a) 传统的梯形腔,(b)新型腔

Fig. 3 Axial field distribution at center gaps and side cavities of two different cavities, (a) the traditional ladder type cavity, (b) the novel cavity

图3 两种腔体在中间间隙和边腔处的轴向场分布,(a) 传统的梯形腔,(b)新型腔

tions (1) and (2), respectively[6], where E_z is the axial field distribution, $\omega = 2\pi f$ is the angular frequency of the mode, W_s is the total energy stored in the resonator (set as 1W in CST), β_e is the propagation constant of the electron beam. The high-frequency characteristic parameters of two cavities defined in Table 1 are listed in Table 2. The novel cavity has almost the same coupling coefficient as the traditional cavity; and the characteristic impedance of the novel cavity is almost twice that of the traditional cavity.

$$R/Q = (\int_{\infty}^{\infty} |E_z| dz)^2/(2\omega W_s) \qquad , \quad (1)$$

Table 1 Parameters of the two cavities
表1 两个腔体的参数

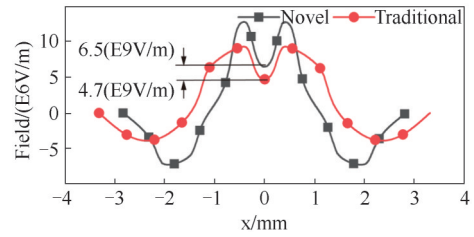| Parameters	Traditional cavity（mm）	Novel cavity（mm）
dr	0. 3	0. 3
cw	2. 4	1. 2
ch	1. 8	1. 8
sw	2. 11	--
sh	2. 8	--
p	0. 9	0. 9
g	0. 25	0. 25
$sw1$	--	0. 8
$sh1$	--	2. 5
$sw2$	--	0. 7
$sh2$	--	2. 0
$sw3$	--	0. 72

Fig. 4 Comparison of transverse electric field distribution between the traditional ladder type cavity and the novel cavity

图4 哑铃型腔和新型腔的横向场对比

Table 2 High−frequency characteristics of the two cavities
表2 两个腔体的高频特性参数

Parameters	Traditional cavity	Novel cavity
Frequency	94.64 GHz	94.61 GHz
M	0.3627	0.3626
R/Q	44.50 Ω	84.6 Ω
M^2R/Q	5.85 Ω	11.12 Ω

$$M = \frac{\int_{\infty}^{\infty} E_z e^{j\beta z} dz}{\int_{\infty}^{\infty} |E_z| dz} \qquad . \quad (2)$$

1. 1 Mode spacing study

For multi-gap resonators, it is necessary to pay attention to the multiple axial modes caused by multiple gaps. N gaps bring N axial modes. These competitive modes need to be far away from the operating mode. During the study, we found that the height of the first side cavity（$sh1$）could control the mode separation and did not change the frequency of the operating mode. Figure 5 shows the effect of the height of the first side cavity（$sh1$）on the mode spacing. As the height of the side cavity decreases, the mode separation between the operating mode and the other two axial modes increases. Moreover, changing $sh1$ hardly changes the frequency of 2π

mode. However，smaller *sh*1 will also make the cavity smaller，which is bad for the heat dissipation of the cavity. In addition，the decrease of *sh*1 does not significantly improve the field in the central gaps，especially when *sh*1 is less than 2. 5 mm. When *sh*1 = 2. 5 mm，the mode interval of 2π mode and π/2 mode is 1. 7 GHz，which is sufficient to avoid mode competition.
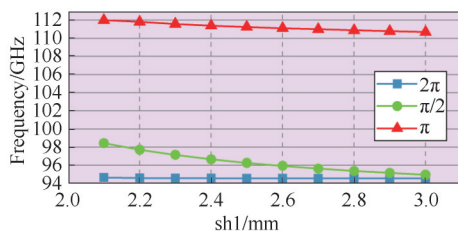

Fig. 5   The resonant frequencies of the three axial modes as a function of *sh*
图5   三个轴向模式谐振频率随 sh 的变化曲线

1. 2   Sensitivity analysis

In the W band，the cavity size becomes very small. Therefore，it is necessary to study dimension sensitivity when designing a cavity. Variations of ±10 μm and ±5 μm have been added to novel cavity models in simulation to see deviations in the resonant frequency. The result is shown in Fig. 6（a）. It can be seen that the resonant frequency is the most sensitive to *ch*1，whereas other sizes are not.

A similar sensitivity analysis has been performed on the traditional cavity defined in Table 1 to give a comparison. The traditional high-order-mode cavity has two sensitive sizes，which are *ch* and *sw*［see Fig. 6（b）］. The most sensitive size is *ch*，which is the height of central gaps. For both the novel cavity and the traditional cavity，when the most sensitive dimension is changed by 5 μm at the same time，the frequency change of the novel cavity is 140 MHz while that of the traditional cavity is 120 MHz. However，it is worth noting that the characteristic impedance of the novel cavity is almost twice that of the traditional cavity［see Table 1］；and the novel cavity has only one sensitive dimension while the traditional cavity has two.

Moreover，the characteristic impedance of resonant cavities plays a key role in determining the circuit efficiency. The effect of fabrication tolerance on novel cavity characteristic impedance has been studied. The result is shown in Fig. 7. In the variation range of ±5 μm，the characteristic impedance varies less than 1 ohm even for the most sensitive size. The 1-ohm variation in characteristic impedance has little effect on circuit efficiency.

2   PIC simulation analysis

An RF circuit operating at the W-band is designed based on the proposed novel multi-gap resonator. Distances between cavities are firstly determined as about 1/4 reduced plasma wavelength and then optimized manually to get the maximum output power. The 3D particle-in-cell （PIC）simulation is done by commercial software CST.
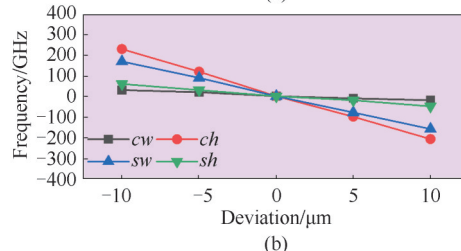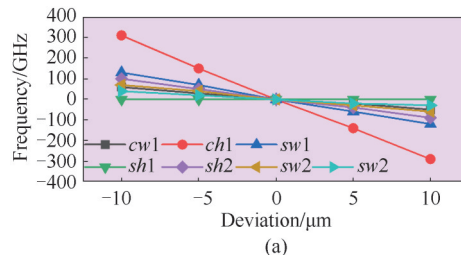

Fig. 6   Effect of dimensional deviation on resonant frequency of two kinds of cavities that operate at TM_{310} mode，（a）the novel cavity，（b）the traditional cavity
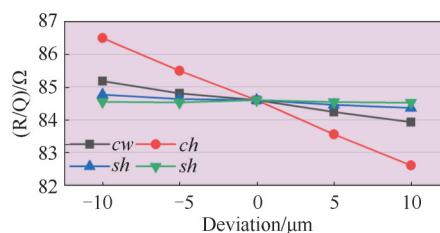图6   不同尺寸偏差对工作在 TM_{310} 模式的两种谐振腔谐振频率的影响，（a）新型谐振腔，（b）传统谐振腔

Fig. 7   Effect of dimensional deviation on the characteristic impedance of the novel cavity that operates at TM_{310} mode
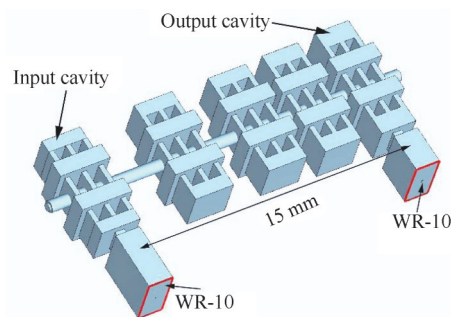图7   不同尺寸偏差对工作在 TM_{310} 模式的新型谐振腔特性阻抗的影响

Fig. 8   Diagram of the interactive circuit
图8   互作用电路示意图

In the PIC model，the oxygen-free high conductivity copper with a conductivity of 5. 8 ×10⁷ *S/m* is assigned to the circuit boundary. A pencil beam with 0. 2 mm radius is injected into the 0. 3 mm radius drift tube. The operating voltage and current of the pencil beam are 25 kV and 2 A respectively. A uniform axial field of 0. 9 T is defined in CST to confine the pencil beam. The magnetic field is twice as strong as the Brillouin field. The Brillouin magnetic field can be given by $B_b = 0. 83 \times 10^{-3} (I_0)^{1/2}/(R_0 (V_0)^{1/4})$，where I_0 is the beam current in

A，R_0 is the beam radius in m，and V_0 is the beam voltage in V. The designed interaction circuit is shown in Fig. 8. The whole interaction circuit consists of five resonators. Each resonator is composed of three gaps to avoid mode competition caused by multiple gaps. The microwave energy input and output of the RF circuit are done by the WR-10 standard waveguides. The parameters of the individual cavities in the interacting circuit are listed in Table 3.

The frequency and the period of the cavity should be carefully designed in order to avoid self-oscillation of the interaction circuit. The whole interacting circuit can be qualitatively analyzed by the equivalent circuit approach. The beam conductance G_e of each resonator is an important parameter to measure the interaction between the field in the resonator and the electron beam. The beam conductance can be given by (3)[15], where $G_0 = I_0/V_0$ and $\beta_e = \omega_q/v_e$. ω_q is the reduced plasma angular frequency. $M(\beta_e - \beta_q)$ and $M(\beta_e + \beta_q)$ are coupling coefficients of fast and slow space charge wave respectively，and they can be calculated from (4) and (5). $E(z)$ is the axial field distribution.

$$G_e/G_0 = \frac{1}{8}\frac{\beta_e}{\beta_q}\left[\left|M(\beta_e - \beta_q)\right|^2 - \left|M(\beta_e + \beta_q)\right|^2\right], \quad (3)$$

$$M(\beta_e - \beta_q) = \frac{\int_\infty^\infty E(z)e^{j(\beta_e - \beta_q)z}dz}{\int_\infty^\infty |E(z)|dz}, \quad (4)$$

$$M(\beta_e + \beta_q) = \frac{\int_\infty^\infty E(z)e^{j(\beta_e + \beta_q)z}dz}{\int_\infty^\infty |E(z)|dz}. \quad (5)$$

Table 3 Optimized parameters of each cavity for the EIK
表3 互作用电路腔体参数

Cavity	f(GHz)	R/Q(Ω)	M	Qe	(R/Q) $M^2(\Omega)$
1	94.78	79.96	0.3660	975	10.71
2	94.70	83.96	0.3627	1196	11.04
3	94.78	83.27	0.3627	1196	10.96
4	94.86	84.44	0.3197	1197	8.63
5	94.66	85.60	0.2865	235	7.02

The RF circuit should be designed such that the beam conductance of the input cavity is greater than zero and that of the output cavity is less than zero. This can be qualitatively explained by the fact that the electron beam absorbs energy as it passes through the input cavity and surrenders energy at the output cavity. The period p of the resonator is an important parameter to characterize the synchronization between the electron beam and the electromagnetic wave. When the velocity of the electron beam is greater than that of the electromagnetic wave,

the electron beam surrenders energy. When the velocity of the electron beam is greater than that of the electromagnetic wave，the electron beam absorbs energy. The period p is 0.9 mm for the first three resonators，0.85 mm for the penultimate cavity，and 0.80 mm for the output cavity. Figure 9 shows the curve of the beam conductance of several cavities as a function of the electron beam voltage. The designed operating voltage is 25 kV. The beam conductance of the input cavity is greater than zero，while the beam conductance of the penultimate cavity and the output cavity are both designed to be less than zero.
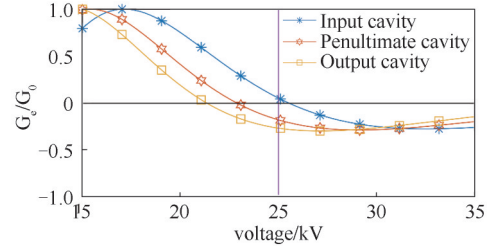

Fig. 9 Normalized beam conductance versus beam voltage of three cavities
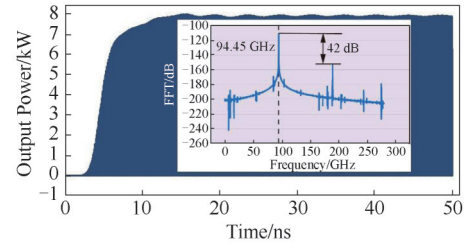图9 三种腔体的归一化电子电导随电子注电压的变化

Fig. 10 Output signal and its frequency spectrum
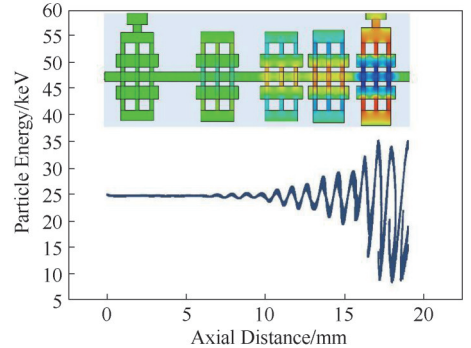图10 输出信号和其频谱

Fig. 11 Particles phase diagram and electric field distribution
图11 粒子相空间图和电场分布

The complete interactive circuit is built in CST. The 3D PIC solver in CST has been used to perform beam-wave interaction simulation. Figure 10 shows the output signal of the interacting circuit and its spectrum. The main frequency of the signal is 94.45 GHz. The output power of the interactive circuit can reach 7.8 kW，and the corresponding electronic efficiency is 15.6%.

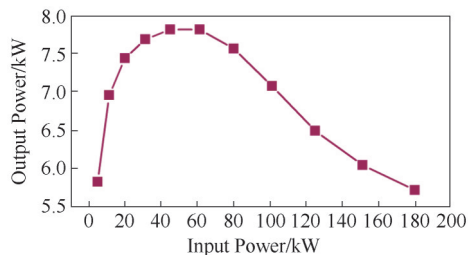Figure 11 shows the phase space diagram of the par-

Fig. 12   Output power vs. input power
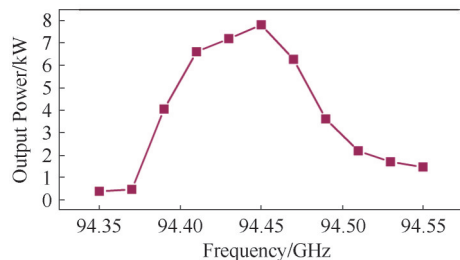图12   输出功率随输入功率的变化曲线

Fig. 13   Frequency sweep curve
图13   频率扫描曲线

ticle when the output signal is stabilized. Moreover, the inset diagram shows the electric field distribution in interactive circuit. As the beam passes through the interactive cavities, the modulation of the beam gradually deeps and the exciting field becomes stronger. Particles slow down at the output cavity and hand over energy to the microwave. The energy of some electrons is below 10 keV. The circuit output power as a function of the input power is shown in Fig. 12. The output power is saturated when the input power is 45 mW, and the saturation gain is 52. 4 dB. The Fourier spectrum single peak in Fig. 10 also demonstrates the purity of the output signal. There is no mode competition in the RF circuit. To get the bandwidth of the interaction circuit, we scan the frequency of the input signal from 94. 35 GHz to 94. 55 GHz with a 0. 02 GHz step. Figure 13 shows the results of the frequency sweep. The 3-dB bandwidth of the RF circuit is 120 MHz. Table 4 gives a comparison of different EIKs. Our EIK demonstrates the highest peak power within EIKs whose operating voltage and current are similar.

3   Conclusions

A novel multi-gap resonator has been proposed for klystrons operating at TM_{310} mode. It has a higher characteristic impedance than the traditional high-order mode cavity. An interactive circuit based on the novel cavity

has been designed. The circuit can produce an output power of 7. 8 kW when 45 mW input power is injected. The corresponding gain and electronic efficiency are 52. 4 dB and 15. 6%, respectively. The high gain and efficiency of the RF circuit are attributed to the high characteristic impedance of the novel cavity. The output power of the designed pencil beam RF circuit is similar to the sheet beam RF circuit. The proposed resonator can be used in the interactive circuits in other millimeter wave and terahertz bands to decrease the circuit length and improve the circuit gain.

References

[1] Chodorow M, Kulke B. An extended-interaction klystron：Efficiency and bandwidth[J]. *IEEE Transactions on Electron Devices*, 1966, **13**(4)：439-447.

[2] Steer B, Roitman A, Horoyski P, *et al*. Advantages of the Extended Interaction klystron Technology at Millimeter and Sub-Millimeter Frequencies [C]. 2007 IEEE 34th International Conference on Plasma Science (ICOPS), 2007.

[3] Yu D U L, Wilson P B, Kin J S. Design of a high-power sheet beam klystron [C]. 1992 AIP Conference Proceedings, 1992.

[4] Pasour J, Wright E, Nguyen T K, *et al*. Demonstration of a Multikilowatt, Solenoidally Focused Sheet Beam Amplifier at 94 GHz.[J]. *IEEE Transactions on Electron Devices*, 2014, **61**(6)：1630-6..

[5] Gamzina D, Barnett L R, Ravani B, *et al*. Mechanical Design and Manufacturing of W-Band Sheet Beam Klystron[J]. *IEEE Transactions on Electron Devices*, 2017, **64**(6)：2675-2682.

[6] Shin Y M, Wang J X, Barnett L R, *et al*. Particle-In-Cell Simulation Analysis of a Multicavity W-Band Sheet Beam Klystron [J]. *IEEE Transactions on Electron Devices*, 2011, **58**(1)：251-258.

[7] Nguyen K T, Pasour J A, Antonsen T, *et al*. Intense Sheet Electron Beam Transport in a Uniform Solenoidal Magnetic Field [J]. *IEEE Transactions on Electron Devices*, 2009, **56**(5)：744-752.

[8] Booske J H, Mcvey B D, Antonsen T M. Stability and confinement of nonrelativistic sheet electron beams with periodic cusped magnetic focusing[J]. *Journal of Applied Physics*, 1993, **73**(9)：4140-4155.

[9] Lopin M I, Pobedonostsev A S, Sazonov B V. High-power multiple beam TWTs and the TWT-based amplifying chains [C]. 1992 IEEE MTT-S Microwave Symposium Digest, 1992.

[10] Gelvich E A., Borisov L M., Zhary Y V, *et al*. The new generation of high-power multiple-beam klystrons [J]. *Microwave Theory and Techniques*, IEEE Transactions on Electron Devices, 1993, **41**(1)：15-19.

[11] Pobedonostev A S , Gelvich E A , Lopin M I , *et al*. Multiple-beam microwave tubes [C]. International Microwave Symposium Digest. IEEE, 1993.

[12] LÜ Su-Ye, ZHANG Chang-Qing, WANG Shu-Zhong, *et al*. Stability Analysis of a Planar Multiple-Beam Circuit for \$W\$-Band High-Power Extended-Interaction Klystron[J]. *IEEE Transactions on Electron Devices*, 2015, **62**(9)：3042-3048.

[13] Dobbs R, Roitman A, Horoyski P. 9.2：Fabrication techniques for a THz EIK[C]. IEEE International Vacuum Electronics Conference, 2010.

[14] WANG Dong-Yang, WANG Guang-Qiang, GUO Jian, *et al*. A high-order mode extended interaction klystron at 0.34 THz.[J]. *Physics of Plasmas*, 2017, **24**(2)：1-8.

[15] Chodorow M, Wessel-Berg T. A High-Efficiency Klystron with Distributed Interaction[J]. *IRE Transactions on Electron Devices*, 1961, **8**(1)：44-55.

Table 4   Performance comparison of different EIKs
表4   EIK 参数对比

Ref	f/GHz	Voltage/kV	Current/A	Bandwidth/MHz	Peak power/kW	Efficiency/%
[4]	94	20	4	100	7. 5	8. 6
[6]	94. 5	74	3. 6	150	50	18. 8
[14]	342. 4	15	0. 3	300	0. 06	1. 3
This work	94. 45	25	2	120	7. 8	15. 6